Letter

Geochemical Perspectives Letters

Textural and chemical inheritance during a pseudomorphic double mineral transformation

P. Forjanes, J.P.H. Perez, C. Berryman, M. Syczewski, L.G. Benning

Supplementary Information

The Supplementary Information includes:

- Description of the Starting Materials, Reagents and Replacement Experiments
- In-depth Description of the Methods Used to Characterize the Materials
- Supplementary Tables S-1 to S-4
- Supplementary Figures S-1 to S-11
- Supplementary Information References

Description of the Starting Materials, Reagents and Replacement Experiments

The reactions that govern two consecutive mineral replacement reactions have been evaluated in this study: (i) the conversion of gypsum single crystals ($CaSO_4 \cdot 2H_2O$) into celestine ($SrSO_4$); and (ii) the subsequent transformation of the replaced crystals into strontianite ($SrCO_3$). For the first replacement reaction, 30 individual natural gypsum single crystals (Teruel, Spain; Crystals C1 to 30; Table S-1 and Fig. S-1; ~25-35 mg per crystal; sizes of approx. 5 x 5 x 2 mm) were placed into 1.5 mL polypropylene (PP) tubes and reacted with 1 mL of a Sr-rich fluid (~0.5 M $SrCl_2 \cdot 6H_2O$; Sigma Aldrich) during increasing reaction times (between 1 minute and 1 day; Table S-1). One day was chosen because in previous experiments this duration was shown to be long enough to fully replace a single crystal with celestine (Forjanes *et al.*, 2020). At specific time points, the crystals were removed from the fluid, washed with mQ water, dried on absorbent paper to remove excess fluid, and left to dry overnight in a preheated oven at 40 °C to remove moisture. To study the second mineral replacement reaction, another set of 30 gypsum crystals (Crystals C31 to 60; Table S-1 and Fig. S-2) were reacted with the Sr-rich solution for one day to convert them into celestine. The so-transformed crystals were removed from the first fluid, dried overnight, and transferred into new PP tubes, where 1 mL of a carbonate-rich fluid (~ 0.5 M Na_2CO_3; Sigma Aldrich) was added. These 2nd set of transformation experiments were also carried out for time periods between 1 minute and 1 day (Table S1), after which the resulting crystals were removed and dried. A full detailed description of the starting materials and chemical reagents used for the two transformation experiments is given below.

Starting Material. Transparent gypsum single crystals ($CaSO_4 \cdot 2H_2O$) from Teruel (Spain). The crystals were cut with a razor blade parallel to $\{010\}_{Gp}$, one of the most common forms of gypsum (Kostov and Kostov, 1999). The weight of each crystal was approximately 25 to 35 mg.

Reagent used for the 1st replacement reaction: Strontium chloride hexahydrate ($SrCl_2 \cdot 6H_2O$) Sigma Aldrich CAS No: 10025-70-4 prepared in MiliQ water (18.2 MØ).

Reagent used for the 2nd replacement reaction: Sodium carbonate concentrate (Na_2CO_3) Sigma Aldrich CAS No: 497-1 prepared in MiliQ water (18.2 MØ).

In-depth Description of the Methods Used to Characterize the Materials

For each interaction time, three crystals were used. Following the reactions, one crystal was grounded in an agate mortar and use for mineral identification by means of powder X-ray diffraction (pXRD). The measurements were performed using a STOE STADI P diffractometer equipped with a Cu X-ray source, a curved Ge (111) monochromator and a MYTHEN2 detector in flat plate transmission geometry. The obtained diffraction patterns were analysed using the PROFEX software for phase identification (Doebelin and Kleeberg, 2015). The same powder used for pXRD was subsequently used for Fourier transformed infrared (FTIR) spectroscopy, where a ThermoFisher Nicolet iS5 spectrometer with KBr optics and an iD7 single-reflection diamond ATR accessory was used. For each measurement, 64 spectra with a resolution of 4 cm^{-1} were coadded. The replacement reaction progress was monitored using scanning electron microscopy (SEM) on polished sections of the second interacted crystal. To prepare these sections, the crystals were embedded in epoxy resin (Teexpert) in silicone moulds, ensuring that the $(010)_{Gp}$ face was perpendicular to the base of the mould. The resin blocks were then manually polished in 8 steps (P320 to P2000) until highly polished sections were obtained. SEM was also used to image the surfaces of the reacted crystals using the third crystal after interaction with the solutions. Both polished sections and whole-crystals were mounted on sample holders and coated with 20 nm of carbon (Leica EM ACE600). The surfaces of the interacted crystals were imaged with secondary electrons (SE) while the polished sections were imaged with backscattered electrons (BSE) using a FEI Quanta 3D Dual Beam scanning electron microscope operated at 5 kV (20 kV for EDS analysis).

For the chemical characterization of the crystals and the reacting fluids, additional experiments were carried out in which 150 mg of crystals were interacted with 15 mL of solution in order to keep the fluid: solid ratio of the experiments described above. At different time-points of the experiments, the crystals (following full-digestion) and the supernatant fluids were analyzed by inductively coupled plasma optical emission spectrometry (ICP-OES). For this purpose, about ~25–35 mg of gypsum, celestine and strontianite fragments from each experimental round and selected interaction times were digested using acid-cleaned Erlenmeyer flasks, and reacted with 10 mL of boiling aqua regia ($HCl:HNO_3$ = 3:1) until completely dissolved. After cooling to room temperature, the digests were quantitatively transferred to acid cleaned volumetric flasks and made up to 100 mL with ultrapure water (Milli-Q, ~18.2 MΩ·cm). Meanwhile, supernatant liquid samples collected from the time-resolved reactions solutions were filtered through 0.2-µm polyethersulfone (PES) syringe filters. Filtrates were collected in acid-cleaned polypropylene (PP) tubes and then acidified with HNO_3 (Aristar® for trace analysis, VWR). Prior to analysis, acidified liquid samples (pH ~2) were diluted gravimetrically in acid-cleaned polypropylene (PP) tubes. Sample dilutions were done using 0.3 M HNO_3. Dilution factors ranging from 500 to 10,000 were adapted to ensure that the analyte solutions were within the concentration range of the matrix-

matched calibration standards (linearity criteria $R^2 > 0.99990$). Elemental concentrations were determined using a SPECTROGREEN inductively coupled plasma optical emission spectrometer (ICP-OES, SPECTRO Analytical Instruments) equipped with dual side-on interface (DSOI) plasma observation. Concentrations of Ca, Na, S, and Sr in the samples were evaluated using the emission wavelengths of 317.933, 589.592, 180.731 and 421.552 nm, respectively. For each analytical session, instrumental stability and drift were monitored using Ar at emission wavelengths of 420.067 nm for each sample analysis and regular measurements of a quality control (QC) solution. Instrumental statistical limits of detection (LOD = 3 SD above background) and limits of quantification (LOQ = 10 SD above background) were determined in each analytical session based repeat analysis (n = 5) of 0.3 M HNO_3 used for sample dilution. Analytical uncertainties at a 95 % confidence level for concentrations quantified (above LOQ) during this study are <2 % relative, verified by repeat analyses of the QC solution (n = 5) (Table S2). Due to the high concentrations of S in the fluid, this element could be analysed by ICP-OES. It can be assumed that all the S present in the solution is sulfate coming from the dissolution of the starting gypsum, as the initial fluid is S-free. The composition of the digested phases in wt. % plotted in Figs. 1 and 2) was obtained quantitatively from the raw ICP data.

To determine the changes in specific surface area and the development of porosity during the different successive mineral replacement experiments, gas sorption analyses were carried out using nitrogen as adsorbate. Prior to measurements, reacted crystals (~1 g in total) were evacuated at room temperature for 16 h, followed by degassing at 80 °C under vacuum for 4 h using a VacPrep™ 061 Sample Degas System (Micromeritics®). This temperature of 80 °C is low enough to avoid the dehydration of the gypsum starting material as this transformation has extremely slow kinetics for temperatures below ~100 °C (Charola *et al.*, 2007 and references therein). After degassing, the specific surface area (SSA) was measured by N_2 sorption at 77 K in a Gemini VII Surface Area and Porosity analyser (Micromeritics®). SSA was calculated using the Brunauer–Emmett–Teller (BET) equation (Brunauer *et al.*, 1938) and applying the Rouquerol criterion (Rouquerol *et al.*, 2007). The uncertainty of the measurement is ~1.3 % based on repeat analysis (n = 3, relative SD = 0.66 %) of a certified reference material (alumina, 004-16858-00) that we measured as $SSA_{BET} = 5.13 \pm 0.03$ m^2 g^{-1}.

Supplementary Tables S-1 to S-4

Table S-1 Experiments carried out in this work. The first 30 crystals (C1 to C30) were used to study the time-resolved transformation of gypsum single crystals into celestine after increasing interaction times with a Sr-rich solution. The next 30 crystals (C31 to C60) were first transformed into celestine within 1 d of interaction with the Sr-rich solution and then transformed into strontianite by reacting them with a carbonate-rich fluid.

Crystal Name	Interaction with … (Round 1) *Gypsum to Celestine*		Crystal Name	Interaction with … (Round 1) *Gypsum to Celestine*		Interaction with … (Round 2) *Celestine to Strontianite*	
	Solution	Time		Solution	Time	Solution	Time
C1 toC3	1 mL of ~ 0.5 M $SrCl_2 \cdot 6H_2O$	1 min	C31 to C33	1 mL of ~ 0.5 M $SrCl_2 \cdot 6H_2O$	24 h	1 mL of ~ 0.5M Na_2CO_3	1 min
C4 to C6		5 min	C34 to C36				5 min
C7 to C9		10 min	C37 to C39				10 min
C10 to C12		30 min	C40 to C42				30 min
C13 to C15		1 h	C43 to C45				1 h
C16 to C18		3 h	C46 to C48				3 h
C19 to C21		6 h	C49 to C51				6 h
C22 to C24		12 h	C52 to C54				12 h
C25 to C27		18 h	C55 to C57				18 h
C27 to C30		24 h	C58 to C60				24 h

Table S-2 ICP-OES data for quality control solutions (QC) that were prepared from single element standard solutions (Merck, CertiPur) to achieve chemical compositions similar to the experimental sample solutions. The mean results of n replicate analyses are given together with the standard deviation (SD) and relative standard deviation (RSD) (SD represents 68 % of the population, 2SD represents 95 % of the population). The measured deviation from QC is a quantitative estimation of accuracy.

	Elemental concentration (mg L^{-1})			
	Ca	Na	S	Sr
Wavelength (nm) *Instrumental limits* (n = 7)	317.933	589.592	180.731	421.552
Limit of detection (LOD)	0.001	0.005	0.004	0.008
Limit of quantification (LOQ) *Quality control* (*QC*, n = 8)	0.003	0.015	0.011	0.024
Measured concentration	0.676	0.669	0.664	0.676
SD	0.002	0.005	0.002	0.003
RSD	0.30 %	0.76 %	0.32 %	0.44 %
2RSD	0.61 %	1.53 %	0.64 %	0.87 %
QC concentration	0.665	0.665	0.656	0.659
Measured deviation from QC	1.71 %	0.71 %	1.18 %	2.45 %

Table S-3 Crystal composition and mole fraction of acid digested crystals obtained at varying reaction times during the mineral replacement experiments. Prior to acid digestion, crystals were washed with Milli-Q water to remove unreacted salts deposited on crystal surfaces. The composition of the crystals in mM was obtained from the raw ICP data in ppm.

Reaction	Time (h)	Crystal composition [wt. %]				Mole fraction in crystal (x)	
		Ca	Sr	S	Na	Ca (x_{Ca})	Sr (x_{Sr})
Gypsum to Celestine	0	23.5 ± 0.5	-	18.4 ± 0.3	-	1.000	-
	0.167	22.0 ± 0.2	2.3 ± 0.4	18.0 ± 0.1	0.12 ± 0.07	0.955	0.045
	1	18.1 ± 0.2	9.9 ± 0.1	17.8 ± 0.2	0.15 ± 0.06	0.800	0.200
	3	13.8 ± 0.6	18.0 ± 1.2	17.3 ± 0.1	0.15 ± 0.03	0.627	0.373
	18	1.9 ± 0.2	40.9 ± 0.4	16.5 ± 0.2	0.26 ± 0.16	0.091	0.909
	24	1.0 ± 0.8	42.5 ± 1.1	16.5 ± 0.3	0.20 ± 0.19	0.051	0.949
Celestine to Strontianite	0	1.0 ± 0.8	42.5 ± 1.1	16.5 ± 0.3	0.20 ± 0.19	0.051	0.949
	0.167	0.65 ± 0.25	43.3 ± 0.7	15.5 ± 0.1	0.41 ± 0.03	0.032	0.968
	1	0.38 ± 0.06	45.1 ± 0.6	12.3 ± 0.6	0.63 ± 0.03	0.018	0.982
	3	0.73 ± 0.60	46.5 ± 2.0	7.7 ± 2.0	1.1 ± 0.3	0.033	0.967
	18	1.8 ± 1.9	47.1 ± 2.0	2.9 ± 2.0	1.5 ± 0.2	0.077	0.923
	24	0.59 ± 0.23	51.9 ± 0.1	0.51 ± 0.08	1.7 ± 0.1	0.024	0.976

Table S-4 Concentration of elements released to the reactive fluid during the mineral replacement experiments. The composition of the fluids in mM was obtained from the raw ICP data in ppm.

Reaction no. 1	Time (h)	Elements released to the fluid				Reactive fluid
		Ca_{fluid} (mM)	$Ca_{release}$ (%)	S_{fluid} (mM)	$S_{release}$ (%)	Sr_{fluid} (mM)
Gypsum to Celestine	0	*bdl*	-	*bdl*	-	462 ± 2
	0.167	2.9 ± 0.2	5.1 ± 0.2	0.27 ± 0.12	0.5 ± 0.2	462 ± 1
	1	12.7 ± 0.7	22.9 ± 1.6	0.56 ± 0.12	1.0 ± 0.2	452 ± 2
	3	22.1 ± 1.2	40.6 ± 2.3	0.94 ± 0.44	1.8 ± 0.8	444 ± 1
	18	53.9 ± 1.9	97.4 ± 1.9	0.66 ± 0.15	1.2 ± 0.2	418 ± 1
	24	54.6 ± 2.0	98.6 ± 3.5	0.83 ± 0.18	1.5 ± 0.3	417 ± 4
Reaction no. 2	**Time (h)**	**Elements released to the fluid**				
		Sr_{fluid} (nM)	$Sr_{release}$ (%)	S_{fluid} (mM)	$S_{release}$ (%)	Ca_{fluid} (nM)
Celestine to Strontianite	0	*bdl*	-	*bdl*	-	*bdl*
	0.167	9 ± 2	0.017 ± 0.003	4.1 ± 0.2	9.0 ± 0.3	41 ± 1
	1	7 ± 1	0.016 ± 0.001	15.6 ± 1.9	30.8 ± 3.6	40 ± 4
	3	6 ± 1	0.013 ± 0.002	27.2 ± 2.6	51.0 ± 5.1	37 ± 1
	18	4 ± 1	0.009 ± 0.001	49.0 ± 2.5	93.5 ± 4.7	21 ± 6
	24	4 ± 1	0.008 ± 0.001	54.6 ± 0.5	99.4 ± 1.4	17 ± 2

Supplementary Figures S-1 to S-11

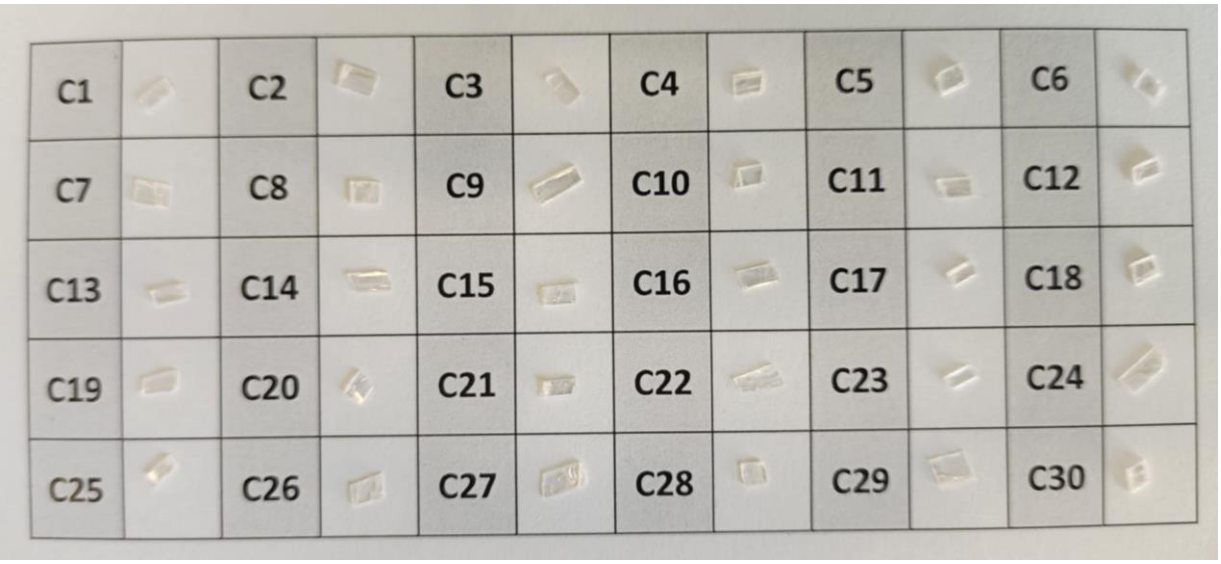

Figure S-1 Crystals 1 to 30 used to study the transformation of gypsum into celestine before the beginning of the interaction. The crystals were reacted with $SrCl_2 \cdot 6H_2O$ for progressively longer interaction times. The starting crystals are transparent natural gypsum single crystals and the size of each square in which the gypsum crystals are placed is 1 cm^2.

Figure S-2 Crystals 31 to 60 used to study the transformation of gypsum into celestine and then to strontianite before the beginning of the first interaction experiments.

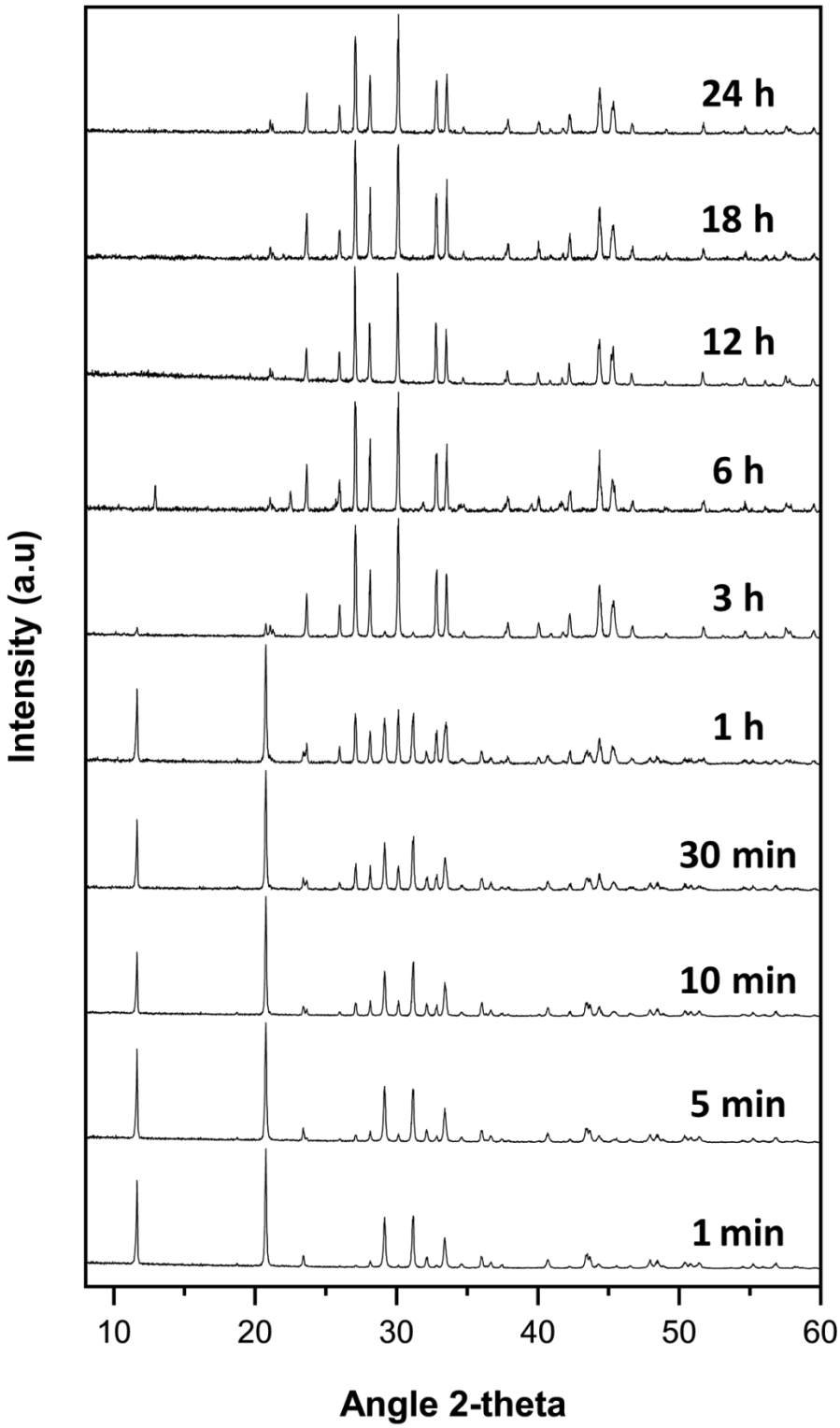

Figure S-3 pXRD patterns of reacted gypsum single crystals following their reaction with a Sr-bearing fluid showing their complete replacement by celestine within 1 day.

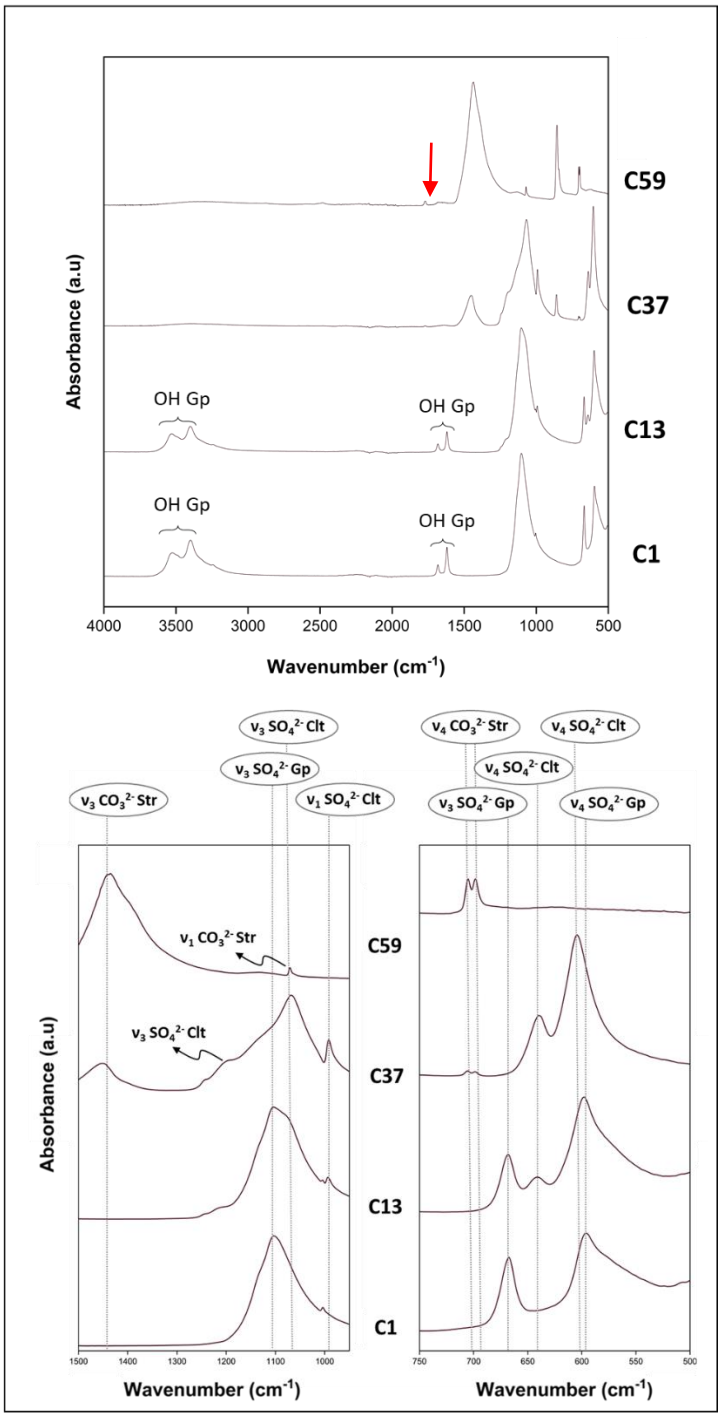

Figure S-4 FTIR data are consistent with pXRD results and show that, upon interaction with a Sr-rich solution, gypsum is transformed into celestine (C1 and C13). In the second stage, the interaction of celestine with carbonate-rich fluids triggers the subsequent replacement by strontianite (C37 and C59). The broad band at ~1100 cm^{-1} in the strontianite crystals (red arrow in the pattern of crystal C59) suggests that this phase may incorporate minor amounts of sulfate, which is consistent with the ICP-OES data of the solid (Table S-3).

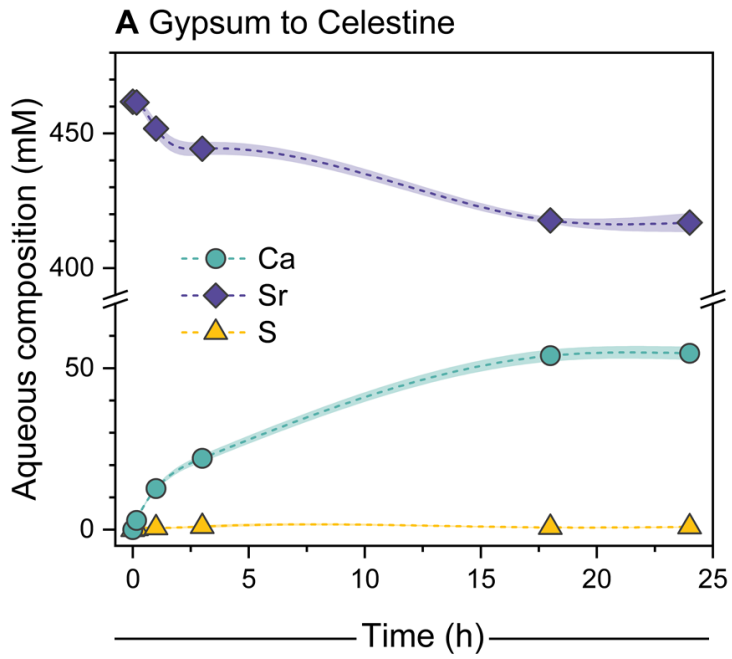

Figure S-5 Evolution of the aqueous composition of Sr-reacting fluids during the 1st transformation experiments, where gypsum crystals were reacted with Sr-rich fluids. Measurements obtained by ICP-OES.

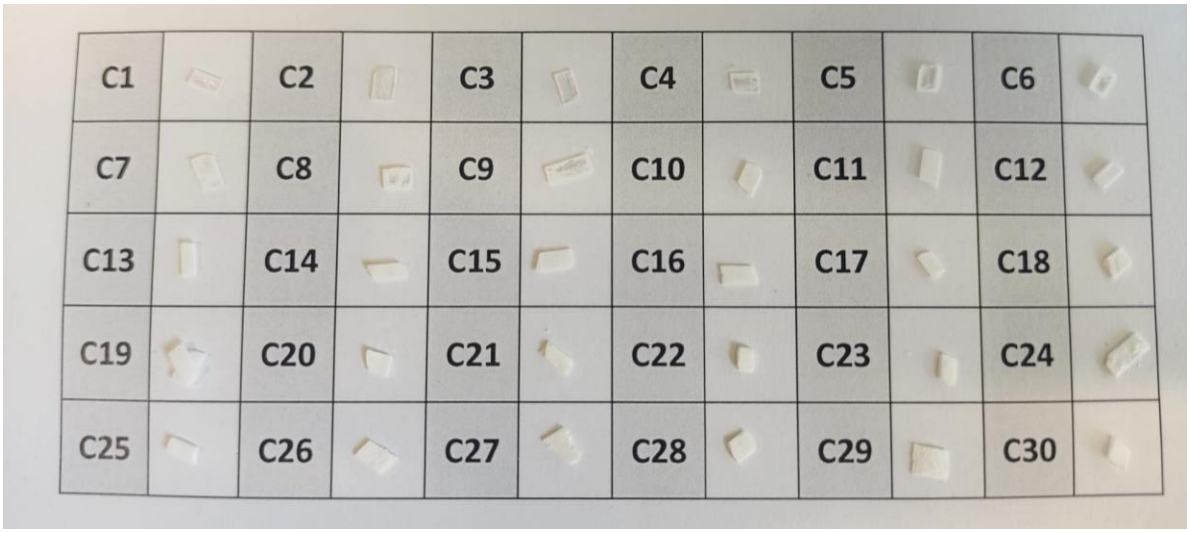

Figure S-6 Crystals 1 to 30 after increasing interaction times with the Sr-rich solution (between 1 minute and 1 day). The interaction leads to the replacement of the gypsum crystals by celestine aggregates. The replacement has a pseudomorphic character: the external shape of the gypsum crystal is preserved during the transformation to celestine and is accompanied by a colour change from transparent to white.

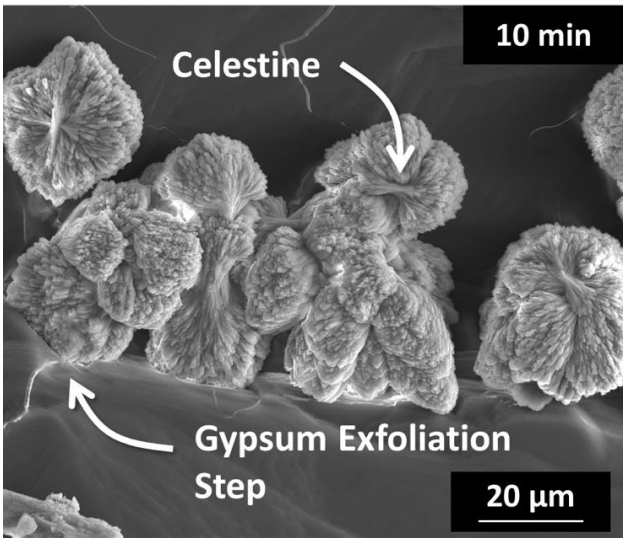

Figure S-7 Celestine crystals initially grow in the vicinity of the exfoliation steps of the gypsum parent surfaces.

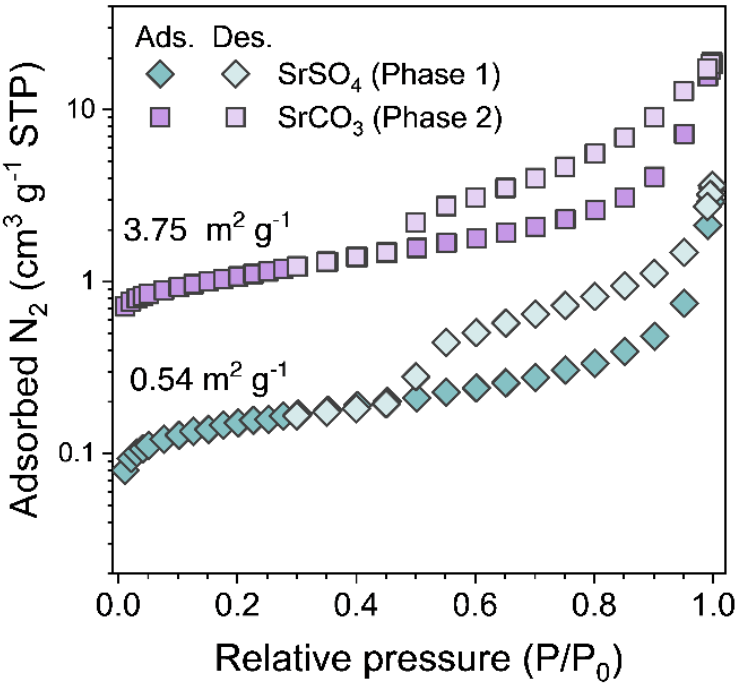

Figure S-8 Nitrogen sorption isotherms of celestine ($SrSO_4$, diamonds) and strontianite ($SrCO_3$, squares) obtained at 77 K. Dark coloured symbols denote the adsorption branch while the light-coloured symbols indicate the desorption branch. No isotherms could be measured for the initial large gypsum crystals, implying a <0.01 m^2/g SSA. The N_2 adsorption isotherms of both celestine ($SrSO_4$; teal diamonds) and strontianite ($SrCO_3$; purple squares) are classified as Type II isotherms, indicating unrestricted monolayer-multilayer adsorption of N_2 molecules on the mineral surfaces. N_2 sorption analysis on gypsum did not yield an isotherm, which denotes extremely low SSA_{BET} values (<0.01 $m^2\ g^{-1}$). The SSA_{BET} of celestine and strontianite were determined to be **0.54** and **3.75 $m^2\ g^{-1}$**, respectively. This corresponds to a 7-fold increase in the surface area of the crystals after the 2nd phase transformation. The hysteresis curve (light coloured symbols) is indicative of a Type H3 loop, suggesting the presence of a pore network consisting of macropores (pore sizes >50 nm).

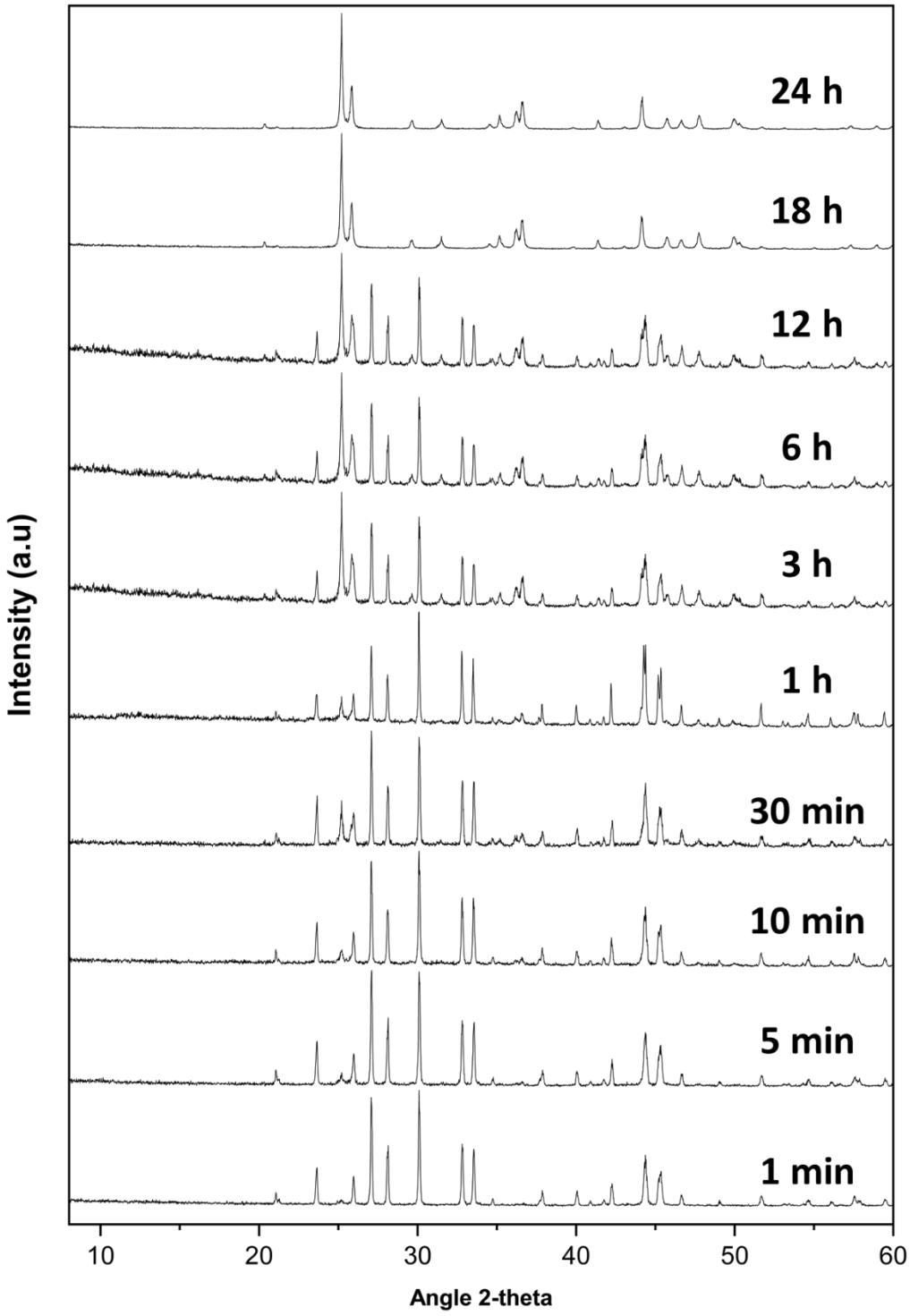

Figure S-9 Complete diffractograms of the celestine pseudomorphs after increasing interaction times with a solution bearing carbonate. The interaction results in a complete replacement of the pseudomorph by strontianite within 1 day.

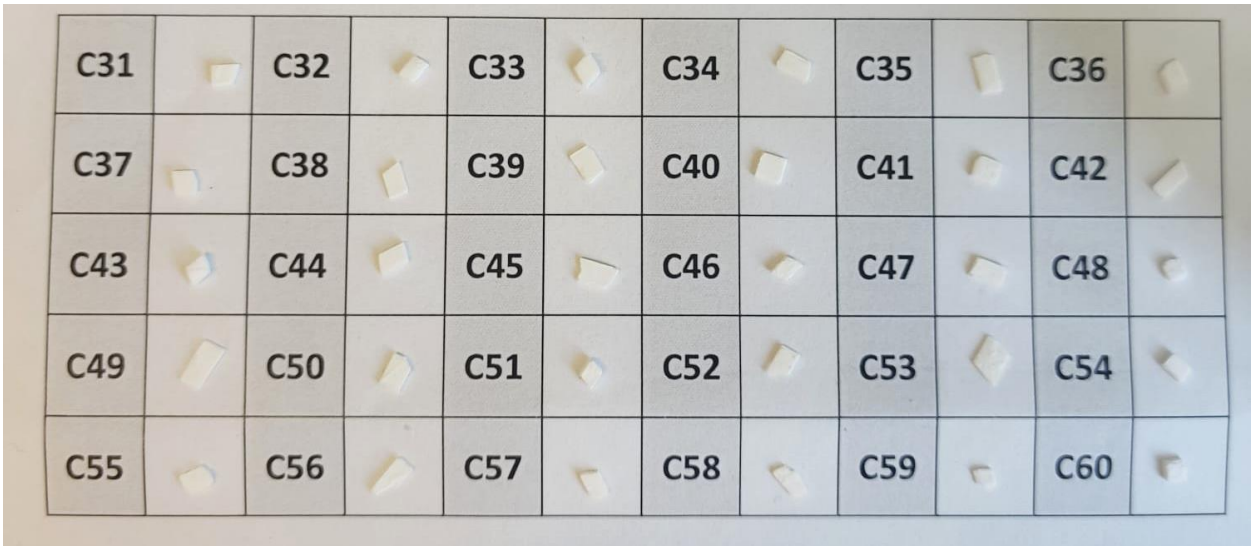

Figure S-10 Crystals 31-60 after the 2 rounds of transformation. All these crystals were interacted with the Sr-rich solution for one day to completely transform them into celestine. They were then interacted with the carbonate-rich solution during increasing interaction times (1 min to 1 day) to study their subsequent transformation into strontianite. The original external morphology of the gypsum precursor single crystals was maintained all the time.

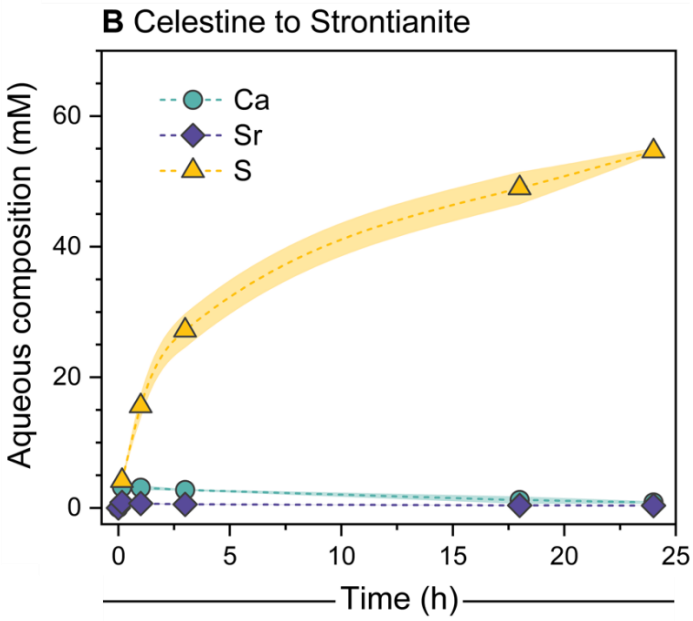

Figure S-11 Evolution of the composition of carbonate-rich fluids after interaction with celestine pseudomorphs during increasing interaction times. Measurements obtained by ICP-OES.

Supplementary Information References

Brunauer, S., Emmett, P.H., Teller, E. (1938) Adsorption of Gases in Multimolecular Layers. *Journal of the American Chemical Society* 60, 309–319. https://doi.org/10.1021/ja01269a023

Charola, A.E., Pühringer, J., Steiger, M. (2007) Gypsum: A review of its role in the deterioration of building materials. *Environmental Geology* 52, 339–352. https://doi.org/10.1007/s00254-006-0566-9

Doebelin, N., Kleeberg, R. (2015) *Profex*: A graphical user interface for the Rietveld refinement program *BGMN*. *Journal of Applied Crystallography* 48, 1573–1580. https://doi.org/10.1107/S1600576715014685

Forjanes, P., Astilleros, J.M., Fernández-Díaz, L. (2020) The Formation of Barite and Celestite through the Replacement of Gypsum. *Minerals* 10, 189. https://doi.org/10.3390/min10020189

Kostov, I., Kostov, R.I. (1999) *Crystal Habits of Minerals*. Academic Publishing House, Sofia.

Rouquerol, J., Llewellyn, P., Rouquerol, F. (2007) Is the BET equation applicable to microporous adsorbents? In: Llewellyn, P.L., Rodriquez-Reinoso, F., Rouqerol, J., Seaton, N. (Eds.) *Characterization of Porous Solids VII: Proceedings of the 7th International Symposium on the Characterization of Porous Solids (COPS-VII), Aix-en-Provence, France, 26-28 May 2005*. Elsevier, Amsterdam, *Studies in Surface Science and Catalysis* 160, 49–56. https://doi.org/10.1016/s0167-2991(07)80008-5